RESEARCH

Zerumbone ameliorates the inflammatory response and organ damage in severe acute pancreatitis via the ROS/NF-κB pathway

Fengmei Zhang[1] and Dongjia Xu[1*]

Abstract

Objective The aim of the current study was to determine the mechanism by which Zerumbone (ZER) ameliorates inflammation and organ damage in a rat model of severe acute pancreatitis (SAP).

Methods Different concentrations of ZER (10, 20 and 40 mg/kg) were administered by femoral vein puncture 30 min prior to establishment of the SAP model. Hematoxylin and eosin (H&E) staining was used to assess pathological changes in the pancreatic tissue of SAP-induced rats. The lung wet/dry (W/D) ratio was assessed and serum levels of amylase (AMY), alanine aminotransferase (ALT), creatinine (Cr), aspartate aminotransferase (AST) and phospholipase A_2 (PLA_2) were measured. Western blot analysis was used to examine changes in the expression of ROS/NF-κB pathway-associated proteins.

Results SAP was confirmed by significant histopathological damage to the pancreas. ZER (10, 20 and 40 mg/kg) was found to alleviate pancreatitis and decrease ascites volume, lung W/D ratio, pancreatic pathology score, oxidative stress and inflammatory damage. High concentrations (20 and 40 mg/kg) of ZER were shown to increase levels of hepatorenal toxicity. In contrast, 10 mg/kg ZER was found to attenuate liver enzyme levels, reduce pathological damage to the liver, and protect against extrapancreatic organ damage to the liver in SAP-induced rats. Moreover, ZER showed no significant side effects in normal rats. Finally, we demonstrated that ZER mediated its anti-inflammatory effects on SAP through the ROS/NF-κB signaling pathway.

Conclusion ZER alleviated SAP-induced oxidative stress and inflammatory injury via the ROS/NF-κB pathway, and had a protective effect on lung injury and liver damage.

Keywords Zerumbone, Severe acute pancreatitis, Organ damage, ROS, NF-κB

*Correspondence:
Dongjia Xu
zhangfengmei123_1@163.com
[1]Department of Gastroenterology, Haining People's Hospital,
Jiaxing City 314400, Zhejiang, China

Introduction

Acute pancreatitis (AP) is an inflammatory disease that is characterized by the activation of pancreatic enzymes, which leads to the digestion, edema, hemorrhage and even necrosis of pancreatic tissue. Clinical manifestations of SP include acute abdominal pain, abdominal distension, nausea, vomiting, fever and elevated blood pancreatic enzymes. In particular, severe acute pancreatitis (SAP) is diagnosed when patients with AP develop multiple complications including pancreatic hemorrhage and necrosis, secondary infection, peritonitis and shock with persistent organ failure (>48 h). Statistical evidence indicates that AP progresses to SAP in 10–20% of patients [1–5]. Due to the rapid onset and progression of the disease, SAP is associated with a relatively high mortality rate and overall poor prognosis.

Although inflammatory responses, oxidative stress injury, apoptosis and microcirculatory disorders have been shown to contribute to the activation of trypsin, the pathogenesis of SAP remains unclear. Recent studies have shown that activation of pancreatic enzymes may also lead to excessive secretion of inflammatory factors and the necrosis of pancreatic tissues, thereby contributing to the development of complications including liver and lung damage [6, 7]. Therefore, in clinical practice, a treatment regimen for SAP involving fasting and early enteral nutrition was designed to prevent further deterioration of symptoms. However, this treatment did not significantly improve the overall condition of SAP patients [8, 9]. Several studies have shown that combining traditional Chinese medicine with the above treatment regimen shortens the course of the disease, reduces the possibility of developing complications and improves the overall prognosis of patients, by protecting the intestinal mucosa and reducing the systemic inflammatory response of the patients [10].

ZER is the main active ingredient in the extract of *Zingiber zerumbet (L.) smith* (a traditional Chinese medicine), and has been reported to possess anti-inflammatory and oncological properties, which are mediated through inhibition of the PI3K-mTOR, MAPK-ERK, NF-κB and NF-κB/TLR signaling pathways [11–15].

Although previous studies have reported that ZER can alleviate the damage caused by SAP [16], the underlying mechanism remains unknown. Since the ROS/NF-κB pathway may be involved in the development of various diseases including immune system disorders, cardiovascular diseases and inflammatory diseases [17–21], we hypothesized that ZER may exert its anti-inflammatory effects through the ROS/NF-κB pathway. Therefore, in the present study, we examined whether ZER alleviated histopathological damage, inflammation and oxidative stress levels, and adjacent organ damage in SAP-induced rats through the ROS/NF-κB pathway in order to provide a reference for the clinical prevention and treatment of SAP.

Materials and methods

Animals

Thirty-six male SPF-grade Wistar rats, weighing 200−250 g and aged 8–10 weeks, were purchased from Beijing baiaosike Biomedical Technology Co., Ltd. All rats were acclimatized and kept for 7 days at a room temperature of 22−24 ℃ and relative humidity of 50–60% in animal housing with free access to standard chow and sterile distilled water. The study was approved by the Experimental Animal Ethics Committee of Beijing baiaosike Biomedical Technology Co., Ltd ethics committee (No. MDL 2023-02-11-01).

Establishment of the SAP model

Prior to construction of the SAP model, rats had unrestricted access to food and water. Rats were then weighed and randomly assigned to groups. Rats were anaesthetized by intraperitoneal injection of 10% chloric acid hydrate (0.3 mL/100 g; PM12563, Perfemiker, Shanghai, China) solution. Once anaesthetized, the limbs and incisors were fixed with a rubber band, and the animals were placed onto the operating table, where their skin was prepared and disinfected. After covering the rats with a sterile towel sheet, a median incision was made into the upper abdomen to expose the duodenum and pancreaticobiliary duct. The pancreaticobiliary duct was double clamped near the hilar with a noninvasive vascular clamp, and the duodenum was pierced with a scalp needle (diameter of 0.4 mm). A retrograde puncture of the cholangiopancreatic duct was then performed through the duodenal papilla. The needle was fixed in position with a noninvasive vascular clamp, and freshly prepared 5% sodium taurocholate solution (0.1 mL/100 g; T0875, Sigma-Aldrich, USA) was injected into the biliopancreatic duct at a constant speed (0.1 mL/min). Next, the scalp needle was removed and the vascular clamp remained in position for a further 5 min to allow the sodium taurocholate solution to fully enter each pancreatic lobule. After 5 min, the vascular clamp was loosened. Congestion and edema of the pancreatic tissue, as well as the duodenum, were observed by the naked eye. Then, the abdomen was closed in layers. Finally, rats were injected subcutaneously with normal saline.

Animal grouping and drug intervention

Thirty-six SPF male rats were randomly assigned to the following six groups (n=6): normal control group (control), SAP group, ZER (471-05-6, Kingherbs, Changsha, China) treatment group (10, 20, 40 mg/kg) group and ZER drug control group (40 mg/kg ZER). A rat model of SAP was established as described earlier. The control

group was treated the same as the SAP group, except rats were injected into the biliopancreatic duct with normal saline instead of 5% sodium taurocholate solution. The ZER control group was treated the same as the normal control group, except 40 mg/kg of ZER was administered by femoral vein puncture 30 min prior to saline injection. The ZER treatment groups were administered different concentrations of ZER by femoral vein puncture 30 min prior to induction of SAP.

Sample collection

Twelve hours post-SAP, blood (approximately 3 mL) was drawn by cardiac puncture with a 5 mL syringe, centrifuged at 3000 rpm/min for 15 min in a high speed centrifuge, and the supernatant was collected and stored at -20 °C in EP tubes. Rat ascites was absorbed with dry cotton balls. Pancreatic tissue was removed from rats in each of the treatment groups, fixed with 4% paraformaldehyde for 24 h, dehydrated in gradient alcohol, soaked in xylene and embedded in paraffin. The lung wet-to-dry (W/D) ratio was measured using the middle lobe of the right lung of the rats. The formula for calculating the amount of ascites was the weight of wet cotton ball - weight of dry cotton ball [22].

Hematoxylin and eosin (H&E) staining

After treatment, rats were humanely killed by cervical dislocation, and pancreatic tissue was quickly isolated, fixed in 10% neutral formaldehyde solution, paraffin-embedded, sectioned and stained with H&E. Histopathological damage to the pancreas was then visualized and photographed.

Pulmonary W/D ratio

The middle lobe of the right lung was isolated. Blood and water were cleaned from the surface of the lung tissue with absorbent paper. The lung tissue was wrapped in aluminum foil (3×3 cm^2 square) and weighed on an electronic scale (wet lung weight). Then, the lung tissue was placed in an oven at 70 °C for 24 h and reweighed to give a value for the dry weight. The W/D ratio was calculated using the following formula: W/D ratio=wet weight of lung - weight of tinfoil / dry weight of lung - weight of aluminum foil.

Measurement of pancreatic biochemical parameters

Pancreatic tissue stored in liquid nitrogen was added to prechilled saline (4ºC) at a ratio of 1:9, homogenized, and the supernatant was collected, divided and frozen. SOD, MDA, NO, GSH and GST levels in the pancreatic tissue were determined spectrophotometrically according to the instructions of the corresponding kits. The kits were purchased from Wuhan Saipei Biotechnology Co., Ltd (Wuhan, China) and are as follows: SP12914 for SOD, SP30131 for MDA, SP13028 for NO, SP12673 GSH, and SP12891 for GST.

ELISA

Following treatment, 4 mL of blood was drawn from the abdominal aorta of the rats, centrifuged at 3000 rpm for 10 min and the supernatant was collected. Levels of serum amylase (AMY), alanine aminotransferase (ALT), creatinine (Cr), aspartate aminotransferase (AST), phospholipase A$_2$ (PLA$_2$), TNF-α, IL-1β, IL-6, IL-4 and IL-10 were measured using the corresponding ELISA kits according to the manufacturer's instructions. The ELISA kits were purchased from Shanghai Zhen Ke Biological Technology Co., Ltd. (Shanghai, China) and are as follows: ZK-6864 for AMY, ZK-6809 for ALT, ZK-7219 for AST, ZK-6963 for Cr, ZK-6363 for PLA$_2$, ZK-6601 for TNF-α, ZK-5809 for IL-1β, ZK-5835 for IL-6, ZK-5838 for IL-4, and ZK-5858 for IL-10. Briefly, the following step was necessary to obtain the levels of indicators measured above. Prepared diluted antibody was incubated with coating buffer overnight at 4℃. After determining the number of experimental wells, standards, samples with buffer were added to each well (depending on the types of wells). Antibodies were added and incubated at room temperature, experimental plates were washed and pre-diluted enzymes were added and incubated. Color development was carried out using TMB and the reaction was terminated by adding stop solution. Finally, OD values were read and analyzed using Curve Expert.

Western blot analysis

Total protein was extracted from pancreatic tissue using lysis buffer. Protein samples were separated by SDS-PAGE, then transferred to PVDF membranes by the wet transfer method. Membranes were incubated in 5% skimmed milk powder at 37°C for 2 h. Next, membranes were incubated with antibodies against p65 (1:1,000; ab76302, Abcam, Cambridge, UK), p-p65 (1:1,000; ab43041, Abcam), I-κBα (1:1,000; ABP55384, AmyJet Scientific, Wuhan, China), p-I-κBα (1:1,000; HK5704, Shanghai Tusi Medical Technology Co., Shanghai, China), Keap1 (1:1,000; ab218815, Abcam), Nrf2 (1:1,000; ab31163, Abcam) and GAPDH (1:2,000; ab8245, Abcam) at 4 °C overnight. The next day, membranes were incubated with HRP-labelled secondary antibodies (1:2,500) at room temperature for 1 h. Protein bands were analyzed by ImageJ and quantified relative to GAPDH.

Immunofluorescence staining

Paraffin tissue Sect. (4 μm) were dewaxed. Antigen retrieval was performed using 0.01 mol/L sodium citrate. Then, endogenous peroxidase was eliminated from the tissue by dropwise addition of 3% catalase. Next, samples were incubated with 5% BSA for 1 h, then incubated

overnight at 4 °C with a primary antibody against Keap1 (1:100 dilution; added dropwise).

Statistical analysis

Data were analyzed using SPSS 20.0 statistical software. Statistical data are presented as the average±SD. One-way ANOVA was used to compare groups, while LSD was used for two-way comparisons. Then, $\alpha = 0.05$ was considered to be statistically significant.

Results

ZER pretreatment alleviates pathological tissue damage in SAP-induced rats

H&E staining revealed normal pathological changes in the pancreas of control rats, with almost no edema, hemorrhage and inflammatory cell infiltration (Fig. 1A,B). In contrast, pathological changes were observed in the SAP group, including enlarged glandular cells, destruction of normal tissue structure, significant necrosis of the glandular alveoli, typical fat necrosis in some regions, significant inflammatory cell infiltration in the pancreatic lobules, significant inflammatory cell exudation from blood vessels and an increased pathological damage score (Fig. 1A,B). Notably, intravenous administration of ZER (10, 20 and 40 mg/kg) led to a reduction in pancreatic edema, alveolar necrosis, extravascular and septal hemorrhage and inflammatory cell infiltration compared to the SAP group (Fig. 1A). In addition, a concentration-dependent reduction in the pathological damage score was observed (Fig. 1B). No significant differences in pancreatic tissue pathology were observed between the drug control and control groups (P<0.05, Fig. 1A,B). The W/D ratio of lung tissue in the SAP group was significantly higher than the control group. Treatment with ZER led to a concentration-dependent decrease in the W/D ratio of lung tissues compared to the SAP group (P<0.05, Fig. 1C). Serum AMY levels and abdominal water volumes were significantly higher in the SAP group than the control group. ZER treatment (10, 20 and 40 mg/kg) led to a significant dose-dependent decrease in AMY and abdominal water levels compared to the SAP group. No significant differences in serum AMY levels and abdominal water volumes were found between the drug control and control groups (P<0.05, Fig. 1D,E). In addition, significantly higher serum ALT levels were observed in the SAP group compared to the control group. Treatment with 10 mg/kg ZER led to a significant reduction in serum ALT levels compared to the SAP group, while 40 mg/kg ZER resulted in significantly higher serum ALT levels. No significant differences in serum ALT levels were observed between the ZER (20 mg/kg) and SAP groups, and drug control and control groups (P<0.05, Fig. 1F). Serum Cr levels were significantly higher in the SAP group compared to the control group. Treatment

with 10 mg/kg ZER led to a significant reduction in serum Cr levels compared to the SAP group (P<0.05, Fig. 1G).

ZER attenuates oxidative stress injury in SAP-induced rats

Next, we evaluated the effects of ZER on oxidative stress in SAP-induced rats. SAP significantly increased MDA and NO levels, while decreasing SOD, GSH and GST levels compared to controls. However, following ZER treatment, a decrease in MDA and NO levels, and increase in SOD, GSH and GST levels were observed compared to the SAP group (p<0.05, Fig. 2A-E). Western blot analysis revealed upregulated Keap1 and very low Nrf2 expression levels in the SAP group compared to the control group. ZER treatment led to a dose-dependent decrease in Keap1 and increase in Nrf2 expression levels compared to SAP-induced rats (P<0.05, Fig. 2F-H). Our Keap1 immunofluorescence staining data were consistent with these results (Fig. 2I).

ZER attenuates inflammatory damage in SAP-induced rats

Subsequently, the effects of ZER on inflammatory damage in SAP-induced rats were evaluated. Our ELISA data revealed an increase in the levels of the inflammatory cytokines IL-6, IL-1β1 and TNF-α, together with a reduction in IL-4 and IL-10 levels in the SAP group compared to the control group. Following ZER treatment, IL-6, TNF-α and IL-1β levels were reduced and IL-4 and IL-10 levels were increased in a concentration-dependent manner compared to the SAP group (P<0.05, Fig. 3A-E). Our qRT-PCR data were consistent with these findings (P<0.05, Fig. 3F-J).

ZER alleviates liver injury in rats with SAP

We found that ZER (10, 20 and 40 mg/kg) was effective in relieving pancreatitis and reducing the volume of ascites, serum AMY levels and pancreatic pathology score. However, although ZER provided relief from pancreatitis at concentrations of 20 mg/kg and 40 mg/kg, these concentrations were found to be more hepatorenal toxic. Thus, rats were treated with 10 mg/kg ZER for 12 h to determine the effects of ZER on liver injury in SAP-induced rats. H&E staining revealed normal pancreatic tissue pathology in the control group with no cytoplasmic vacuole formation, and no bleeding, necrosis or small granulocyte infiltration. In the SAP group, however, a large number of cytoplasmic vacuoles were formed, the cell boundary became blurred, and hepatic necrosis, neutrophil infiltration, liver capillary congestion and bleeding were apparent. In addition, the central vein was deformed and congested, and the pathological score increased (Fig. 4A,B). After intravenous administration of 10 mg/kg ZER, a reduction in the congestion and hepatic necrosis of the liver tissue was observed compared to
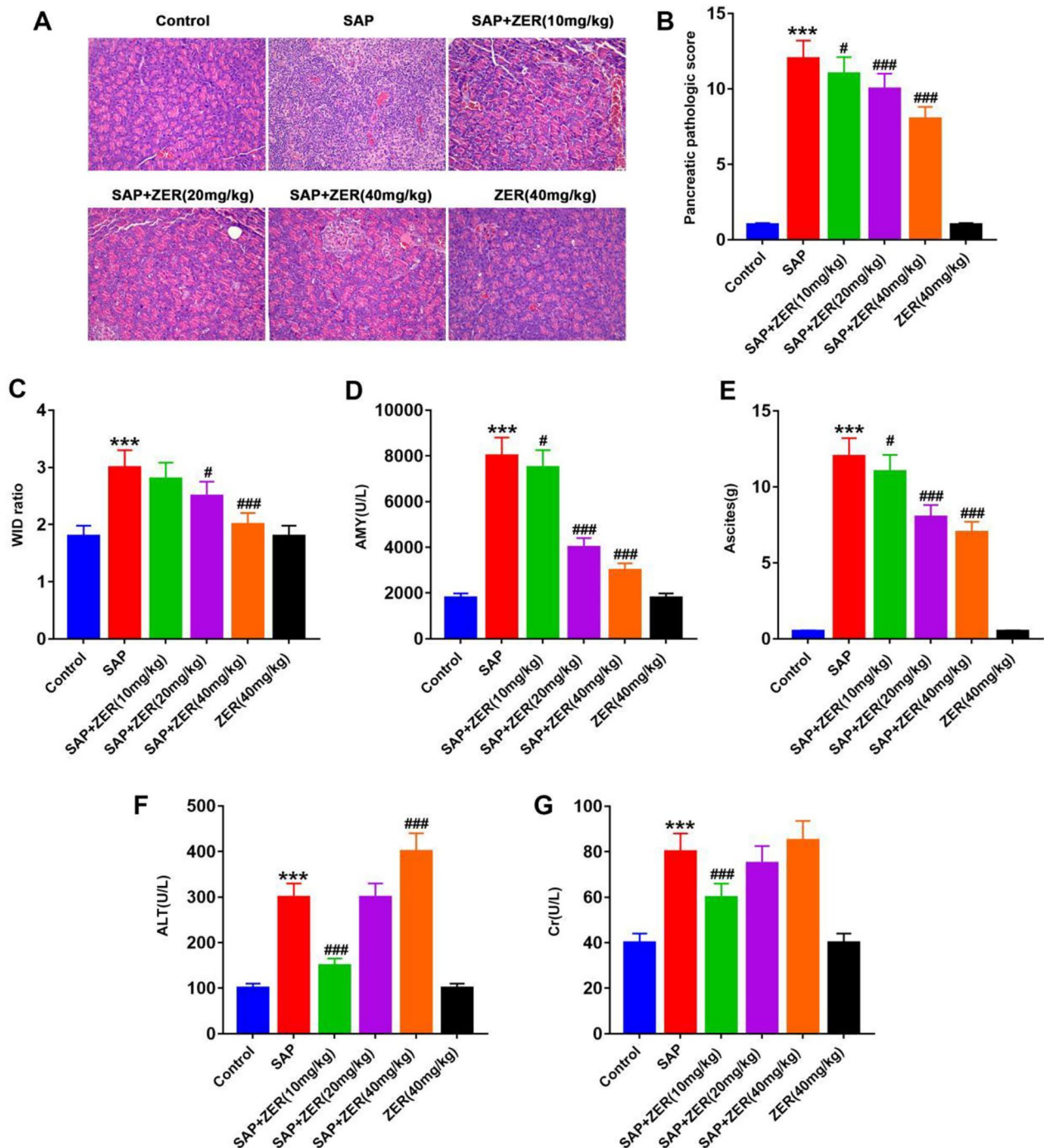
Fig. 1 Pretreatment with ZER alleviates pathological tissue damage in SAP-induced rats. **(A)** Histopathological changes in the rat pancreas of each treatment group were examined by H&E staining (×200). **(B)** Histological score of pancreatic pathology in each group of rats. **(C)** Changes in the wet-to-dry ratio (W/D) of lungs in each group of rats. **(D)** Changes in serum amylase (AMY) levels in each group of rats. **(E)** Measurement of abdominal water volume in each group of rats. **(F)** Changes in serum alanine aminotransferase (ALT) levels in each group of rats. **(G)** Changes in serum creatinine (Cr) levels in rats in each treatment group. ***$P < 0.001$, compared with CON group, #$P < 0.05$, ###$P < 0.001$, compared with the SAP group
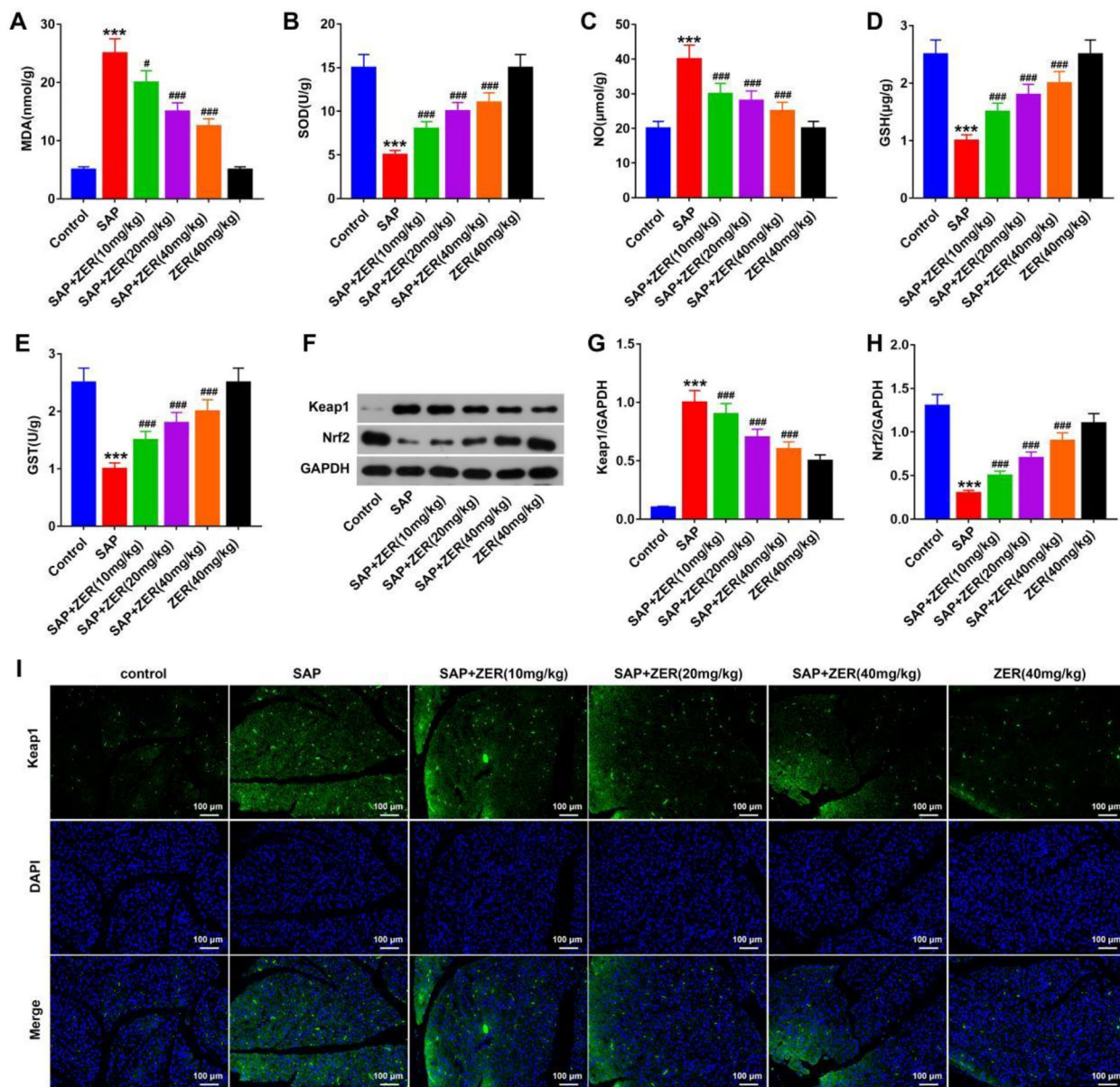
Fig. 2 ZER attenuates oxidative stress injury in SAP-induced rats. **(A-E)** Levels of the oxidative stress factors MDA, SOD, NO, GSH and GST in each group. **(F-H)** Western blot analysis of Keap1 and Nrf2 protein expression levels. (I) Representative immunofluorescence images showing Keap1 staining in the pancreas of each group of rats (scale bar: 25 μm). ***$P < 0.001$, compared with CON group, #$P < 0.05$, ###$P < 0.001$, compared with SAP group

the SAP group. After 12 h, we found that although the morphology of the central vein had returned to normal, some congestion was still observed (Fig. 4A). However, ZER treatment led to a decrease in the pathological score (Fig. 4B). The pathological changes observed in the liver of the ZER drug control (ZER-CON) group were consistent with those in the control group (P < 0.05, Fig. 4A,B). After intravenous administration of 10 mg/kg ZER, the volume of ascites in the ZER group was markedly reduced compared to the SAP group. No significant differences were observed between the ZER-CON and control groups (P < 0.05, Fig. 4C). Next, we evaluated changes

in the serum indices of rats in each treatment group. We found that serum AMY, PLA$_2$, ALT and AST levels in the SAP group were significantly higher than those in the control group. Following intravenous administration of 10 mg/kg ZER, the serum indices in the ZER group were significantly lower than in the SAP group, while no significant differences were found between the ZER-CON and control groups (P < 0.05, Fig. 4D-G).

ZER alleviates SAP through the ROS/NF-κB pathway

Finally, we sought to determine whether the ROS/NF-κB signaling pathway had a role in mediating the effects of
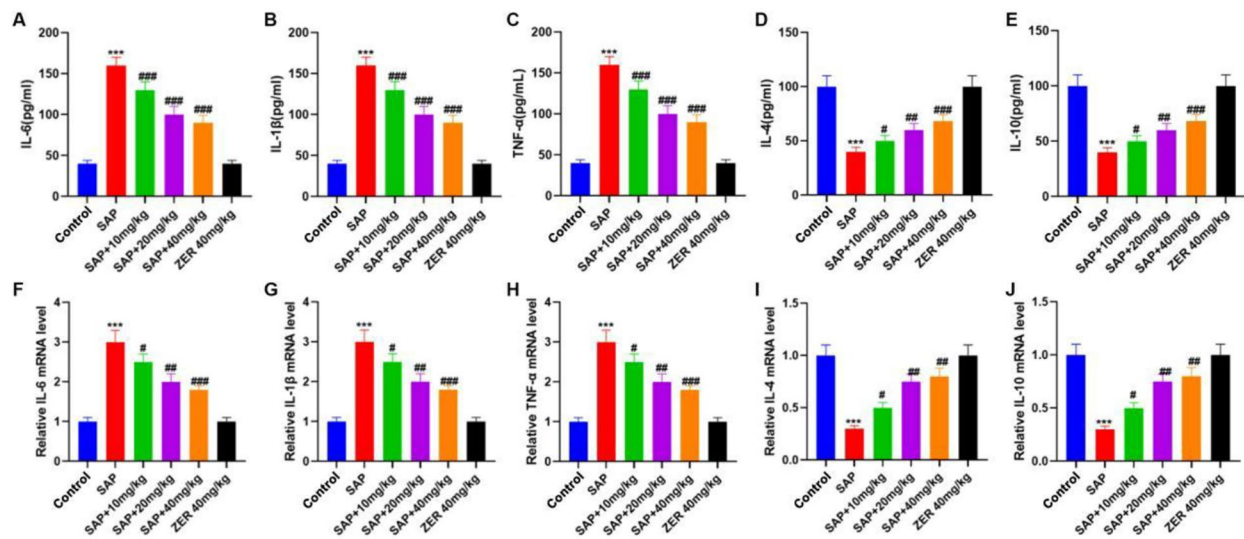
Fig. 3 ZER attenuates inflammatory damage in SAP-induced rats. **(A-E)** ELISA was used to assess the levels of IL-6, IL-1β, TNF-α, IL-4 and IL-10. **(F-J)** The qRT-PCR was used to measure IL-6, IL-1β, TNF-α, IL-4 and IL-10 mRNA levels. ***$P < 0.001$, compared with the CON group, #$P < 0.05$, ##$P < 0.01$, ###$P < 0.001$, compared with the SAP group
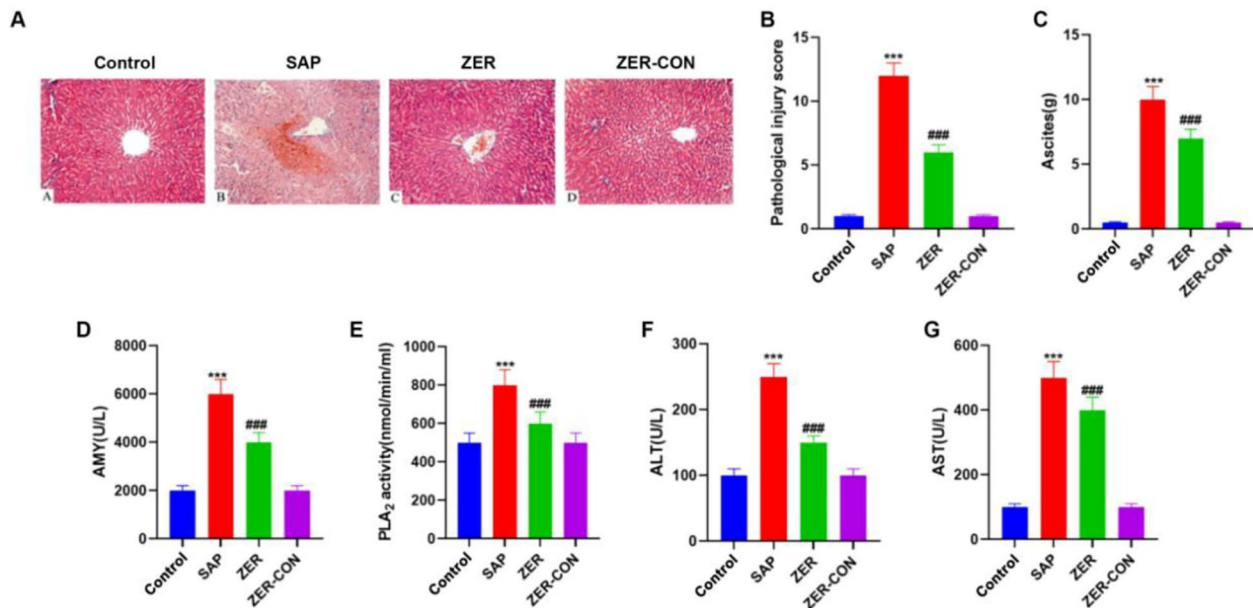

Fig. 4 ZER alleviates liver injury in rats with SAP. **(A)** Histopathological changes in the liver of each group of rats were detected by H&E staining (×200). **(B)** Histological score of the liver pathology for each group of rats. **(C)** Measurement of abdominal water volume in each group of rats. **(D)** Measurement of serum amylase (AMY) levels in each group of rats. **(E)** Determination of serum phospholipase A$_2$ (PLA$_2$) levels in each group of rats. **(F)** Determination of serum alanine aminotransferase (ALT) levels in each group of rats. **(G)** Determination of aspartate aminotransferase (AST) levels in each group of rats. ***$P < 0.001$, compared with the CON group, ###$P < 0.001$, compared with the SAP group

ZER on SAP. The ROS inhibitor NAC was injected intraperitoneally into SAP-induced rats. Our ROS staining data revealed that SAP led to an increase in relative ROS expression levels, while treatment with ZER partially reversed the effects of SAP. NAC was shown to downregulate ROS levels in SAP-induced rats (P < 0.05, Fig. 5A,B). Western blot analysis showed that SAP upregulated the relative expression levels of p65/p-p65 and I-κBα/p-I-κBα in SAP-induced rats, while ZER partially reversed the effect of SAP. NAC was found to downregulate p65/p-p65 and I-κBα/p-I-κBα levels in SAP-induced rats (P < 0.05, Fig. 5C-E).
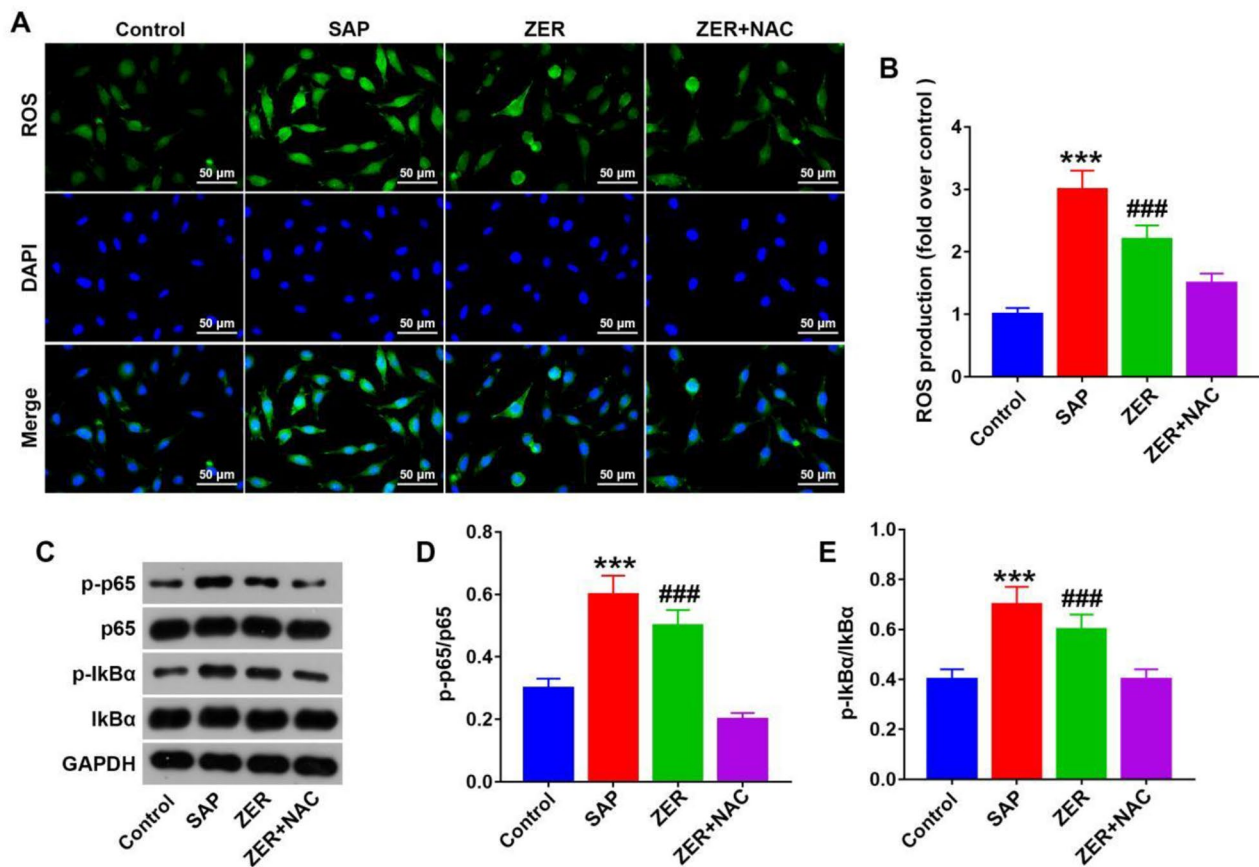
Fig. 5 ZER alleviates SAP through the ROS/NF-κB pathway. **(A,B)** Immunofluorescence staining of ROS levels. **(C-E)** Western blot analysis was used to detect expression of NF-κB pathway-related proteins in each treatment group. Representative western blot and quantification of the western blot data are shown. ***P < 0.001, compared with the CON group, ###P < 0.001, compared with the SAP group.@@@P < 0.001, compared with the ZER group

Discussion

Acute pancreatitis was a disease characterized by acute inflammation of the pancreas and histologic destruction of follicular cells [23]. A severe inflammatory response involving extrapancreatic organs, resulting in organ damage and failure, was indicative of progression to SAP, which had a mortality rate of 20–30% [24, 25]. Epidemiologic evidence suggested that SAP was often associated with hepatic and pulmonary injury, which may be manifested by elevated serum enzyme levels and changes in imaging, and led to a further increased risk of death [26, 27]. Currently, there was no effective treatment for SAP. Therefore, elucidating the pathogenesis of SAP was crucial to improve the overall prognosis of patients!

ZER was a multi-targeted herb with various pharmacological activities including anti-inflammatory and antioxidant properties [16, 28–30]. In the present study, the pathology of the SAP group was characterized by enlarged glandular cells, marked necrosis of the alveolar cells, and typical fat necrosis in some areas, significant inflammatory cell infiltration in the pancreatic lobules and blood vessels, which was consistent with the previous

studies. Meanwhile, the lung W/D ratio in the SAP group was significantly higher than that in the control group. In addition, the levels of serum amylase, ALT, and creatinine were significantly higher in the SAP group along with the amount of ascites. All these results confirmed that the mice had developed SAP.

We compared the difference between the SAP group and the ZER groups at different doses (10, 20 and 40 mg/kg) to investigate the therapeutic effect of ZER on SAP. Our results proved that different doses of ZER were able to alleviate the progression of SAP. Specifically, the ZER groups showed a decrease in ascites volume, lower levels of amylase, ALT and Cr, and a lower pathologic score of pancreatitis. However, there was also a concentration-dependent increase in the hepatorenal toxicity of ZER. Meanwhile, the comparison of ZER control group and Control group indicated that ZER had no significant adverse effects on normal rats. Therefore, ZER at 10 mg/kg was an ideal dose for the treatment of SAP and could serve to alleviate extra-pancreatic organ damage.

The underlying mechanism of ZER in the treatment of SAP remained unclear, and it was reported that SAP

was mainly caused by oxidative stress and the release of inflammatory factors and mediators caused by pancreatic self-digestion [31–37]. Therefore, in the present study, we investigated the changes in the levels of MDA (intermediate product of oxidative stress), NO, SOD and GHS-Px (antioxidant enzymes), IL-6, IL-1β, and TNF-α [38] to investigate the effects of ZER on the levels of oxidative stress and inflammatory factors in rats with SAP. The results showed that the administration of ZER significantly decreased the levels of MDA and NO, and significantly increased the levels of GSH and GST. Meanwhile, the results showed that the levels of IL-6, IL-1β, and TNF-α decreased in a concentration-dependent manner in the ZER group, contrary to the changes in IL-4 and IL-10. Therefore, we demonstrated that ZER could attenuate oxidative stress and inflammatory factor levels in SAP mice. In addition, we verified this finding from the perspective of protein expression. Findings from Western blot showed that ZER led to a reduction in the relative expression levels of p65/p-p65 with I-κBα/I-I-κBα, which was similar to the effect of the ROS inhibitor, NAC. Thus, our results demonstrate that ZER could alleviate SAP through the ROS/NF-κB signaling pathway [39, 40].

However, this study had several limitations, and further in vivo experiments and clinical trials are needed to confirm the role of ZER in regulating ROS/NF-κB in SAP. In conclusion, this study demonstrated that ZER alleviated SAP through the ROS/NF-κB pathway. Thus, ZER may be beneficial in the treatment of SAP.

Supplementary Information

The online version contains supplementary material available at https://doi.org/10.1186/s12876-023-02962-6.

> Supplementary Material 1

Author contributions
FMZ and DJX were involved in material preparation, data collection, and analysis. FMZ wrote the first draft of the manuscript. DJX revised the manuscript carefully. All authors have read and approved the final manuscript.

Data Availability
The datasets used and/or analyzed during the current study are available from the corresponding author upon reasonable request.

Declarations

Ethics approval and consent to participate
Animal experiments were carried out according to the Guidelines of the Animal Experimental Ethics Committee. All methods were carried out in accordance with the relevant guidelines and regulations. All methods are reported in accordance with ARRIVE guidelines for the reporting of animal experiments. The study was approved by the Experimental Animal Ethics Committee of Beijing baiaosike Biomedical Technology Co., Ltd ethics committee (No. MDL 2023-02-11-01).

Consent for publication
Not applicable.

Competing interests
The authors declare no competing interests.

References
1. Portelli M, Jones CD. Severe acute pancreatitis: pathogenesis, diagnosis and surgical management. Hepatobiliary Pancreat Dis Int. 2017;16(2):155–9.
2. Mandalia A, Wamsteker EJ, DiMagno MJ. Recent advances in understanding and managing acute pancreatitis. F1000Res 2018; 7. F1000 Faculty Rev-959.
3. Li ZF, Xu MY, Zhang DH, Gao TT, Gao Z, Li H. Effects of ulinastatin combined with octreotide on blood coagulation function, inflammatory factors and amylase in patients with severe acute pancreatitis. J Biol Regul Homeost Agents. 2020;34(6):2147–51.
4. Li XY, He C, Zhu Y, Lu NH. Role of gut microbiota on intestinal barrier function in acute pancreatitis. World J Gastroenterol. 2020;26(18):2187–93.
5. Fonseca Sepulveda EV, Guerrero-Lozano R. Acute pancreatitis and recurrent acute pancreatitis: an exploration of clinical and etiologic factors and outcomes. J Pediatr (Rio J). 2019;95(6):713–9.
6. Liang X, Hu C, Liu C, Yu K, Zhang J, Jia Y. Dihydrokaempferol (DHK) ameliorates severe acute pancreatitis (SAP) via Keap1/Nrf2 pathway. Life Sci. 2020;261:118340.
7. Fu Q, Zhai Z, Wang Y, Xu L, Jia P, Xia P, et al. NLRP3 deficiency alleviates severe acute pancreatitis and pancreatitis-associated lung injury in a mouse model. Biomed Res Int. 2018;2018:1294951.
8. Majidi S, Golembioski A, Wilson SL, Thompson EC. Acute pancreatitis: etiology, pathology, diagnosis, and treatment. South Med J. 2017;110(11):727–32.
9. Morato O, Poves I, Ilzarbe L, Radosevic A, Vazquez-Sanchez A, Sanchez-Parrilla J, et al. Minimally invasive surgery in the era of step-up approach for treatment of severe acute pancreatitis. Int J Surg. 2018;51:164–9.
10. Yang C, Wang T, Chen J, He J, Li Y, Chen C, et al. Traditional chinese medicine formulas alleviate acute pancreatitis: pharmacological activities and mechanisms. Pancreas. 2021;50(10):1348–56.
11. Su CC, Wang SC, Chen IC, Chiu FY, Liu PL, Huang CH, et al. Zerumbone suppresses the LPS-induced inflammatory response and represses activation of the NLRP3 inflammasome in macrophages. Front Pharmacol. 2021;12:652860.
12. Wang D, Li Y, Cui P, Zhao Q, Tan BB, Zhang ZD, et al. Zerumbone induces gastric cancer cells apoptosis: involving cyclophilin A. Biomed Pharmacother. 2016;83:740–5.
13. Li J, Wang L, Sun Y, Wang Z, Qian Y, Duraisamy V et al. Zerumbone-induced reactive oxygen species-mediated oxidative stress re-sensitizes breast cancer cells to paclitaxel. Biotechnol Appl Biochem 2022.
14. Zainal NS, Gan CP, Lau BF, Yee PS, Tiong KH, Abdul Rahman ZA, et al. Zerumbone targets the CXCR4-RhoA and PI3K-mTOR signaling axis to reduce motility and proliferation of oral cancer cells. Phytomedicine. 2018;39:33–41.
15. Kim A, Gwon MH, Lee W, Moon HR, Yun JM. Zerumbone suppresses high glucose and LPS-induced inflammation in THP-1-derived macrophages by inhibiting the NF-κB/TLR signaling pathway. Nutr Res. 2022;100(3):58–69.
16. Wenhong D, Jia Y, Weixing W, Xiaoyan C, Chen C, Sheng X, et al. Zerumbone attenuates the severity of acute necrotizing pancreatitis and pancreatitis-induced hepatic injury. Mediators Inflamm. 2012;2012:156507.
17. Sousa NA, Oliveira GAL, de Oliveira AP, Lopes ALF, Iles B, Nogueira KM, et al. Novel ocellatin peptides mitigate LPS-induced ROS formation and NF-κB activation in microglia and hippocampal neurons. Sci Rep. 2020;10(1):2696.
18. Sato J, Kinugasa M, Satomi-Kobayashi S, Hatakeyama K, Knox AJ, Asada Y, et al. Family with sequence similarity 5, member C (FAM5C) increases leukocyte adhesion molecules in vascular endothelial cells: implication in vascular inflammation. PLoS ONE. 2014;9(9):e107236.
19. Luo CY, Wei YM, Li SZ, Li CJ, Zheng HL. Anti-inflammatory effect of different solvent extracts from the Rhizome of Imperata Cylindrica on

Lipopolysaccharide-Stimulated RAW264.7 cells. J Biol Regul Homeost Agents. 2022;36(5):1637–46.

20. Huang M, Xin W. Matrine inhibiting pancreatic cells epithelial-mesenchymal transition and invasion through ROS/NF-κB/MMPs pathway. Life Sci. 2018;192(12):55–61.

21. Shi Y, Hua QJ, Li N, Zhao M, Cui Y. Protective effects of evodiamine against LPS-induced acute kidney injury through regulation of ROS-NF- κ B-mediated inflammation. Evid Based Complement Alternat Med. 2019;2019(1):2190847.

22. van Zanden JE, Leuvenink HGD, Verschuuren EAM, Erasmus ME, Hottenrott MC. A translational rat model for ex vivo lung perfusion of pre-injured lungs after brain death. PLoS ONE. 2021;16(12):e0260705.

23. Ortiz Morales CM, Girela Baena EL, Olalla Munoz JR, Parlorio de Andres E, Lopez Corbalan JA. Radiology of acute pancreatitis today: the Atlanta classification and the current role of imaging in its diagnosis and treatment. Radiologia (Engl Ed). 2019;61(6):453–66.

24. Ye S, Si C, Deng J, Chen X, Kong L, Zhou X et al. Understanding the effects of metabolites on the gut microbiome and severe acute pancreatitis. *Biomed Res Int* 2021; 2021:1516855.

25. Shen X, Li WQ. High-mobility group box 1 protein and its role in severe acute pancreatitis. World J Gastroenterol. 2015;21(5):1424–35.

26. Liu W, Du JJ, Li ZH, Zhang XY, Zuo HD. Liver injury associated with acute pancreatitis: the current status of clinical evaluation and involved mechanisms. World J Clin Cases. 2021;9(34):10418–29.

27. Li M, Zhang X, Wang B, Xu X, Wu X, Guo M, et al. Effect of JAK2/STAT3 signaling pathway on liver injury associated with severe acute pancreatitis in rats. Exp Ther Med. 2018;16(3):2013–21.

28. Lee CY, Chen SP, Su CH, Ho YC, Yang ML, Lee SS, et al. Zerumbone from Zingiber zerumbet ameliorates lipopolysaccharide-induced ICAM-1 and cytokines expression via p38 MAPK/JNK-IkappaB/NF-kappaB pathway in mouse model of acute lung injury. Chin J Physiol. 2018;61(3):171–80.

29. Chien TY, Huang SK, Lee CJ, Tsai PW, Wang CC. Antinociceptive and anti-inflammatory effects of zerumbone against mono-iodoacetate-induced arthritis. Int J Mol Sci. 2016;17(2):249.

30. Hemn HO, Noordin MM, Rahman HS, Hazilawati H, Zuki A, Chartrand MS. Antihypercholesterolemic and antioxidant efficacies of zerumbone on the formation, development, and establishment of atherosclerosis in cholesterol-fed rabbits. Drug Des Devel Ther. 2015;9:4173–208.

31. Liu X, Zhu Q, Zhang M, Yin T, Xu R, Xiao W et al. Isoliquiritigenin ameliorates acute pancreatitis in mice via inhibition of oxidative stress and modulation of the Nrf2/HO-1 pathway. *Oxid Med Cell Longev* 2018; 2018:7161592.

32. Huang L, Jiang Y, Sun Z, Gao Z, Wang J, Zhang D. Autophagy strengthens intestinal mucosal barrier by attenuating oxidative stress in severe acute pancreatitis. Dig Dis Sci. 2018;63(4):910–9.

33. Piao X, Sui X, Liu B, Cui T, Qi Z. Picroside II improves severe acute pancreatitis-induced hepatocellular injury in rats by affecting JAK2/STAT3 phosphorylation signaling. *Biomed Res Int* 2021; 2021:9945149.

34. Kong L, Deng J, Zhou X, Cai B, Zhang B, Chen X, et al. Sitagliptin activates the p62-Keap1-Nrf2 signalling pathway to alleviate oxidative stress and excessive autophagy in severe acute pancreatitis-related acute lung injury. Cell Death Dis. 2021;12(10):928.

35. Mei QX, Hu JH, Huang ZH, Fan JJ, Huang CL, Lu YY, et al. Pretreatment with chitosan oligosaccharides attenuate experimental severe acute pancreatitis via inhibiting oxidative stress and modulating intestinal homeostasis. Acta Pharmacol Sin. 2021;42(6):942–53.

36. Yang Z, Ji W, Li M, Qi Z, Huang R, Qu J, et al. Protective effect of nimesulide on acute lung injury in mice with severe acute pancreatitis. Am J Transl Res. 2019;11(9):6024–31.

37. Wang G, Zhang J, Xu C, Han X, Gao Y, Chen H. Inhibition of SOCs attenuates acute lung injury induced by severe acute pancreatitis in rats and PMVECs injury induced by lipopolysaccharide. Inflammation. 2016;39(3):1049–58.

38. Karademir M, Gonul Y, Simsek N, Eser O. The neuroprotective effects of 2-APB in rats with experimentally- -induced severe acute pancreatitis. Bratisl Lek Listy. 2018;119(12):752–6.

39. Dong X, Wang L, Song G, Cai X, Wang W, Chen J, et al. Physcion protects rats against cerebral ischemia-reperfusion injury via inhibition of TLR4/NF-kB signaling pathway. Drug Des Devel Ther. 2021;15:277–87.

40. Sul OJ, Ra SW. Quercetin prevents LPS-induced oxidative stress and inflammation by modulating NOX2/ROS/NF-kB in lung epithelial cells. *Molecules* 2021; 26(22).

Publisher's Note